JOURNAL OF VIROLOGY, Nov. 2003, p. 11312–11323 Vol. 77, No. 21
0022-538X/03/$08.00+0 DOI: 10.1128/JVI.77.21.11312–11323.2003

Coronaviruses as Vectors: Position Dependence of Foreign Gene Expression

Cornelis A. M. de Haan, Linda van Genne, Jeroen N. Stoop, Haukeline Volders, and Peter J. M. Rottier*

Virology Division, Department of Infectious Diseases and Immunology, Faculty of Veterinary Medicine and Institute of Biomembranes, Utrecht University, 3584 CL Utrecht, The Netherlands

Received 21 April 2003/Accepted 5 August 2003

Coronaviruses are the enveloped, positive-stranded RNA viruses with the largest RNA genomes known. Several features make these viruses attractive as vaccine and therapeutic vectors: (i) deletion of their nonessential genes is strongly attenuating; (ii) the genetic space thus created allows insertion of foreign information; and (iii) their tropism can be modified by manipulation of the viral spike. We studied here their ability to serve as expression vectors by inserting two different foreign genes and evaluating systematically the genomic position dependence of their expression, using a murine coronavirus as a model. *Renilla* and firefly luciferase expression cassettes, each provided with viral transcription regulatory sequences (TRSs), were inserted at several genomic positions, both independently in different viruses and combined within one viral genome. Recombinant viruses were generated by using a convenient method based on targeted recombination and host cell switching. In all cases high expression levels of the foreign genes were observed without severe effects on viral replication in vitro. The expression of the inserted gene appeared to be dependent on its genomic position, as well as on the identity of the gene. Expression levels increased when the luciferase gene was inserted closer to the 3′ end of the genome. The foreign gene insertions generally reduced the expression of upstream viral genes. The results are consistent with coronavirus transcription models in which the transcription from upstream TRSs is attenuated by downstream TRSs. Altogether, our observations clearly demonstrate the potential of coronaviruses as (multivalent) expression vectors.

The ability to genetically modify viruses not only has led to extraordinary advances in the understanding of their biology but also has opened a broad new field in which viruses are engineered for use as vaccine vectors and therapeutic agents. The insights in the biological properties of viruses are beginning to allow investigators to rationally modify their pathogenic properties, to provide them with new genetic information, and to retarget them to new cells, tissues, and hosts. Whereas many striking examples have already demonstrated these principles, the true potential of viruses as tools for medical applications has yet to be established. Obviously, the actual prospects will be different for different viruses since these prospects are ultimately determined and limited by the specific features of each virus.

Coronaviruses are enveloped, positive-stranded RNA viruses belonging to the family *Coronaviridae* in the order *Nidovirales*, which also comprises the families *Arteriviridae* and *Roniviridae*. Coronaviruses have the largest known nonsegmented viral RNA genome (up to 31 kb), which is capped, polyadenylated, and infectious (11, 25). The coronavirus genome has its essential genes invariably in the order 5′-replicase-S-E-M-N-3′ and contains, in addition, interspersed among these genes, a varying number of group-specific genes that code for nonstructural proteins (26, 43). These genes, which differ distinctly among the three groups of coronaviruses, were shown to be nonessential for the group 1 coronavirus feline infectious peritonitis virus (FIPV; B. J. Haijema and P. J. M. Rottier, unpublished results) and for the group 2 coronavirus mouse hepatitis virus (MHV) (9).

The replicase domain covers some two-thirds of the genome. It consists of the open reading frames (ORFs) 1a and 1b, which are translated directly from the genomic RNA (gRNA), the more downstream ORF1b by translational read-through using a ribosomal frameshift mechanism. The genes located downstream hereof are expressed from a 3′ coterminal nested set of subgenomic mRNAs (sgRNAs). Except for the smallest one, these sgRNAs are structurally polycistronic but function in general monocistronically since only the 5′-most gene is translated. They all consist of a common leader sequence (65 to 98 nucleotides [nt]), which is identical to the extreme 5′ end of the genome, and a body sequence encompassing various lengths of the genomic 3′ end. Fusion of the leader to the body sequence occurs at transcription regulatory sequences (TRSs; previously named intergenic sequences) that contain a stretch of sequence (nearly) identical to that of the 3′ end of the leader. For MHV, the core consensus TRS is the 9-nt motif 5′-AAU CUAAAC-3′ (11, 25). The sgRNAs are transcribed via a discontinuous transcription mechanism that presumably takes place during negative-strand RNA synthesis, as proposed by Sawicki and Sawicki (39, 40). According to this model, the TRSs serve as transcription termination or pausing signals during negative strand synthesis. Synthesis of the nascent chain resumes either at the same site or after translocation to the leader TRS at the 5′ end. The negative-strand sgRNAs subsequently function as templates for the production of the positive-strand sgRNAs (38, 39, 41, 42).

* Corresponding author. Mailing address: Virology Division, Department of Infectious Diseases and Immunology, Yalelaan 1, 3584CL Utrecht, The Netherlands. Phone: 31-30-2532462. Fax: 31-30-2536723. E-mail: p.rottier@vet.uu.nl.

Since the sgRNAs all have an identical capped 5′ leader sequence, their expression, rather than being regulated at the translation level, is governed primarily by the relative levels of their synthesis. How the transcription levels are regulated is not well understood, but it is clear that the different TRSs play essential roles. Studies have indicated that transcription generally appears to increase with the proximity of the TRS to the 3′ end of the genome (16, 22, 42). Notable exceptions are transmissible gastroenteritis virus (TGEV) and feline infectious peritionitis virus (FIPV), where the smallest sgRNA is synthesized in much smaller quantities than the next smallest sgRNA, which encodes the nucleocapsid (N) protein (7, 42). Because the technologies for manipulating coronavirus genomes have only recently been developed—infectious cDNA clones have been available since 2000 (1, 5, 46, 49, 50)—most of our knowledge of coronavirus transcription comes from studies with defective interfering RNAs (DI-RNAs). These studies showed that the sequence of the TRS itself constitutes part of the signal for sgRNA transcription but that transcription efficiency is also sensitive to changes in the sequences flanking the TRS (2, 3, 9, 10, 15, 19, 21, 28, 29, 32, 33, 47). Insertion of a TRS at different positions in an MHV DI-RNA did not affect its transcriptional activity (19), whereas in a study with a DI-RNA of TGEV higher sgRNA levels were observed when a TRS was placed closer to the 3′ end (2). Another conclusion suggested by various studies is that downstream TRSs have an attenuating effect on the transcription from upstream TRSs (10, 18, 20, 23, 45, 48).

The potential of coronaviruses as vectors has not been studied in any detail. Recent observations have, however, revealed that these viruses have a number of attractive features that might make them very suitable for this purpose. First of all, coronaviruses can be attenuated by the deletion of their nonessential, group-specific genes. This was demonstrated both for MHV (9) and for FIPV. Whereas FIPV normally causes a fatal disease, deletion of the group-specific genes resulted in viruses that were viable but avirulent when inoculated into their natural host (Haijema and Rottier, unpublished). Second, species and tissue specificity of coronaviruses can be modified by manipulation of the targeting function. Thus, MHV was retargeted to feline cells, loosing its ability to infect murine cells, by exchanging the ectodomain of its S protein with that of FIPV S (24); the reverse was demonstrated with FIPV, where the reciprocal exchange generated a feline virus infecting murine cells (14). Similar ectodomain replacements of the S protein led to changes in tissue tropism of MHV (31, 34) and TGEV (12). Third, the conserved genome organization of coronaviruses can be rearranged (10). Deliberate rearrangement of the viral genes will be important to improve the safety of coronaviral vectors since it provides a means to reduce the risk of generating viable viruses by recombination with circulating field viruses. A fourth attractive feature is the unique transcription mechanism of coronaviruses, which allows the expression of foreign genes by simply inserting these genes preceded by a TRS into the coronaviral genome. This principle was already demonstrated by the expression of the green fluorescent protein (GFP) gene from full-length MHV and TGEV genomes (6, 13, 37, 44).

The goal of the present study was to systematically analyze the position dependence of coronavirus foreign gene expression by using MHV as a model. To this end, two unrelated luciferase genes (firefly luciferase [FL] and *Renilla* luciferase [RL]) were inserted at different positions into the MHV genome. An identical TRS was used in all our expression cassettes to allow the direct comparison of the foreign genes by the different recombinant viruses. These viruses were generated by using a convenient method based on targeted recombination and host cell switching (9, 24). The recombinant viruses were analyzed with respect to replication and position dependent expression of their foreign genes.

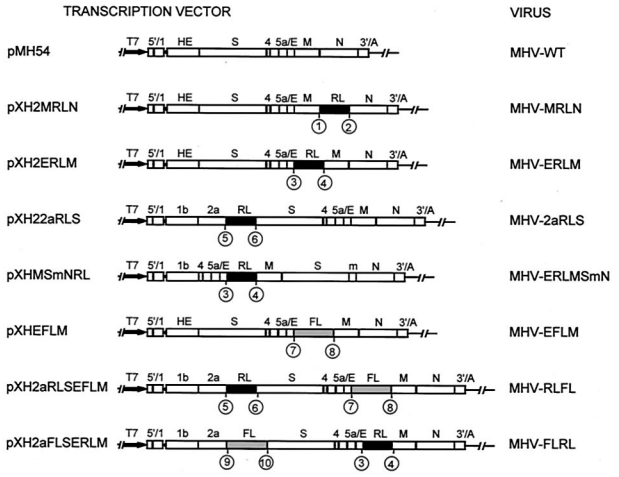

FIG. 1. Plasmid constructs. The transcription vectors from which the defective RNAs were produced in vitro by using T7 RNA polymerase are shown. Vector pMH54 has been described before (24). The other vectors were derived from pMH54 as described in Materials and Methods. The arrow at the left end of each vector indicates the T7 promoter; the solid circle represents the polylinker between the 5′-end segment of the MHV genome (denoted 5′/1) and either the HE gene or the 3′ end of the replicase gene (1b), followed by the structural and group-specific genes and the 3′-untranslated region and the polyadenylated segment (denoted together as 3′/A). The "m" indicates a 126-nt segment from the 3′ end of the M gene. Junctions between viral and insert sequences are marked by numbers in circles; the actual sequences are shown in Fig. 2. The recombinant viruses generated with the transcription vectors are indicated at the right.

MATERIALS AND METHODS

Cells, viruses, and antibodies. LR7 cells (24) were used to propagate the recombinant MHVs (strain A59). The same cells were used for plaque purifications and one-step growth curves. Mouse 17 clone 1 (17Cl1) cells (kindly provided by P. S. Masters) were used for radiolabeling of intracellular viral RNAs. Feline FCWF cells (American Type Culture Collection) were used for infection with the interspecies chimeric coronavirus fMHV (24). The rabbit polyclonal antiserum K134 to MHV A59 has been described previously (36).

Plasmid constructs. Transcription vectors for the production of donor RNA for targeted recombination were derived from transcription vector pMH54 (24) and derivatives thereof. pMH54, which specifies a defective MHV-A59 RNA transcript consisting of the 5′ end of the genome (467 nt) fused to codon 28 of the HE gene and running to the 3′ end of the genome (Fig. 1), was previously used for the construction of a wild-type recombinant virus (MHV-WT) (9). Two reporter genes were used, encoding RL and FL. For both genes, a plasmid was constructed, in which the gene was preceded by an MHV TRS. From this construct the expression cassette (gene plus TRS) could then be transferred into the different transcription vectors (Fig. 1 and 2). As a first step, an MHV TRS was cloned in front of the RL gene. To this end, primer 1286 (5′-GGATATCT AATCTAAACTTTAG-3′) and 1287 (5′-CTAGCTAAAGTTTAGATTAGAT ATCCTGCA-3′) were annealed to each other and cloned into pRL-null (Promega) treated with *Nhe*I and *Pst*I, resulting in pXH1909. For the construction of

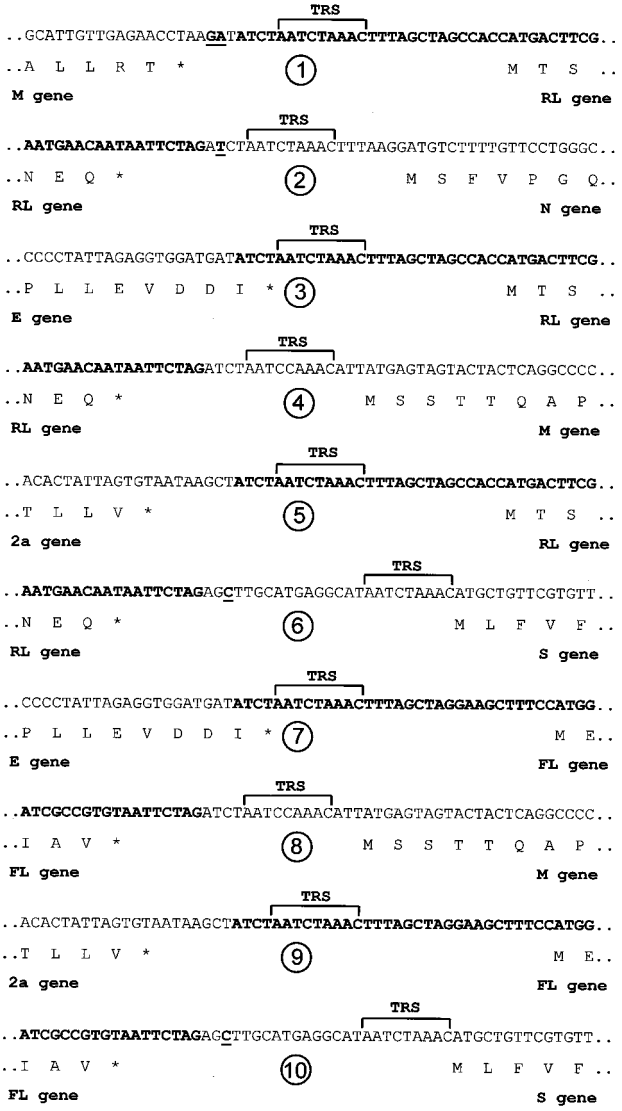

FIG. 2. Sequences at the junctions of the inserted luciferase gene cassettes. Shown are the sequences of the junctions indicated by the circled numbers in Fig. 1. The sequence of the expression cassette is in boldface. Nucleotides outside the expression cassette that differ from the original wild-type MHV-A59 sequence are underlined and in boldface.

the transcription vector containing the RL gene between genes 2a and S (pXH22aRLS, Fig. 1) the following steps were taken. Vector p96 (4), which contains an MHV-A59 cDNA clone, was restricted with *Hin*dIII and *Mlu*I, and the resulting fragment was cloned into pXH1802 (9) treated with *Hin*dIII and *Bss*HII, yielding pXH2103. Next, the RL expression cassette was removed from pXH1909 by restriction with *Eco*RV and *Xba*I, treated with Klenow fragment of DNA polymerase I and cloned into pXH2103, digested with *Hin*dIII, and treated with Klenow fragment, resulting in pXH2509A. Finally, pXH22aRLS (Fig. 1) was constructed by cloning the fragment resulting from digestion of pXH2509A with *Rsr*II and *Avr*II into pMH54 treated with the same enzymes. For the construction of pXH2ERLM, which contains the RL gene between the E and the M genes (Fig. 1), the same expression cassette that was used to make pXH2509A was cloned into pMH54 digested with *Eco*RV. This same expression cassette was also cloned into pXHMeN (10) treated with *Eco*RV, yielding pXH2ERLN. Subsequently, pXH2MRLN, which contains the RL gene between the M and the N genes (Fig. 1), was constructed by cloning the fragment resulting from restriction of pXHMeN with *Eco*RV into pXH2ERLN treated with the same enzyme. pXHMSmNRL was constructed by cloning the RL expression cassette into pXHMSmN (10) treated with *Eco*RV. Thus, pXHMSmNRL (Fig. 1) contains the RL gene between the E and the M gene, but the S gene is placed downstream of the M gene. For the construction of pXHEFLM, which contains the FL gene between the E and the M genes (Fig. 1), the FL gene was first cloned behind the same TRS as was used for the RL expression cassette. To this end, the FL gene was removed from pSP-Luc+ (Promega) by restriction with *Avr*II and *Xba*I and cloned into pXH1909 treated with *Nhe*I and *Xba*I, yielding pXH2711. Subsequently, the FL expresssion cassette was cut out of pXH2711by restriction with *Eco*RV and *Xba*I, treated with Klenow fragment of DNA polymerase I, and cloned into pMH54 restricted by *Eco*RV, resulting in pXHEFLM. In addition, transcription vectors were constructed that contained both the RL and the FL gene. First, pXH2aRLSEFLM (Fig. 1) was constructed, which contains the RL gene between the 2a and the S gene and the FL gene between the E and the M gene, by cloning the FL expression cassette into pXH2aRLS digested with *Eco*RV. Finally, pXH2aFLSERLM (Fig. 1), which contains the RL gene between the E and the M gene and the FL gene between the 2a and the S gene, was engineered. To this end, the luciferase gene was cut out of pSPluc+ (Promega) by restriction with *Xba*I and *Avr*II and cloned into pXH2509A treated with *Xba*I and *Nhe*I to remove the RL gene. The fragment removed from the resulting vector pXH161002 by digestion with RsrII and *Avr*II was cloned into pXHERLM treated with the same enzymes, resulting in pXH2aFLSERLM. All constructs were confirmed by restriction and/or sequence analysis. The sequences of the newly generated junctions indicated in Fig. 1 are shown in Fig. 2.

Generation of recombinant viruses. Incorporation of the expression cassettes into the MHV genome by targeted recombination was carried out as described previously (9, 17). Briefly, donor RNAs transcribed from linearized transcription vectors were electroporated into FCWF cells that had been infected earlier with fMHV. These cells were then plated on a monolayer of murine LR7 cells. After 24 h of incubation at 37°C, progeny viruses released into the culture media were harvested and plaque purified twice on LR7 cells before a passage 1 stock was grown. After confirmation of the recombinant genotypes by reverse transcriptase-PCR (RT-PCR) on purified gRNA, a passage 2 stock was grown that was subsequently used in the experiments.

Radiolabeling of viral RNAs. The metabolic labeling of virus-specific RNAs in infected cells was carried out essentially as reported previously (18, 30). Briefly, 20-cm^2 17Cl1 cell monolayers were infected with each MHV at a multiplicity of infection (MOI) of five 50% tissue culture infective doses ($TCID_{50}$) per cell. At 3 h postinfection, cells were starved in Eagle minimal essential medium containing 5% dialyzed fetal bovine serum (FBS) and 1/10 of the normal phosphate concentration. At 7 h postinfection, cells were labeled for 2 h with either [^{33}P]orthophosphate or [^{32}P]orthophosphate (83 μCi/ml) in phosphate-free Eagle minimal essential medium containing 5% dialyzed FBS and 20 μg of actinomycin D (Sigma) per ml. Total cytoplasmic RNA was purified by using an NP-40 lysis procedure (23), followed by phenol and chloroform extraction and ethanol precipitation. Samples of RNA were denatured with formaldehyde and formamide, separated by electrophoresis through 1% agarose containing formaldehyde, and visualized by fluorography.

Metabolic labeling and immunoprecipitation. LR7 cells were grown and infected with each virus at an MOI of 8. Before being labeled, cells were starved for 30 min in cysteine- and methionine-free minimal essential medium containing 10 mM HEPES (pH 7.2) and 5% dialyzed FBS. The medium was then replaced by 600 μl of the same medium containing 100 μCi of in vitro cell-labeling mix (Amersham). Cells were labeled from 5 to 8 h postinfection. At the end of the labeling period, total lysates were prepared by the addition of 1/4 volume of a fivefold-concentrated lysis buffer to the culture medium (8). Proteins were immunoprecipitated from the lysates as described earlier (8) with 2.5 μl of anti-MHV serum per immunoprecipitation. Immune complexes were adsorbed to Pansorbin cells (Calbiochem) for 30 min at 4°C and were subsequently collected by centrifugation. Pellets were washed four times by resuspension and centrifugation with wash buffers as described earlier (8). The final pellets were suspended in electrophoresis sample buffer. The immunoprecipitates were heated for 2 min at 95°C and analyzed by sodium dodecyl sulfate-polyacrylamide gel electrophoresis (SDS-PAGE) in 15% polyacrylamide gels. Radioactivity in protein bands was quantitated by phosphorscanning of dried gels with a Storm 860 (Molecular Dynamics).

One-step growth curve. LR7 cell monolayers (2 cm^2) were infected at an MOI of 8. At 1 h postinfection, the cells were washed three times with phosphate-buffered saline and then fed with Dulbecco modified Eagle medium supplemented with 10% FBS. Viral infectivity in culture media at different times postinfection was determined by a quantal assay on LR7 cells, and the $TCID_{50}$ values were calculated.

Determination of FL or RL expression. LR7 cell monolayers (2 cm^2) were infected as described above. At the indicated times the culture media were removed, and the cells were lysed by using the appropriate buffer provided with the firefly, *Renilla*, or dual luciferase assay systems (Promega). Intracellular luciferase expression was measured according to the manufacturer's instructions, and the relative light units (RLU) were determined with a LUMAC biocounter M2500 luminometer.

RESULTS

Recombinant MHVs expressing different luciferase genes. Our systematic analysis of coronavirus foreign gene expression started with the incorporation into the MHV genome of two unrelated luciferase genes, which differ distinctly in size (RL [936 nt] and FL [1,653 nt]), taking advantage of the opportunity to differentially detect and quantitate their expression in a simple, extremely sensitive, and technically identical way. As a control we used a reconstructed recombinant wild-type MHV-A59 (MHV-WT), which had been prepared previously (9) by using transcription vector pMH54 (24). This transcription vector encodes defective RNAs composed of the genomic 5′ 467 nt fused to the 3′end of the genome (ca. 8.6 kb) (Fig. 1). The luciferase genes were inserted into similar transcription vectors in the form of expression cassettes. An expression cassette consisted either of a RL or a FL gene, each preceded by an identical TRS (5′-AATCTAAAC-3′) (Fig. 2). In each case the TRS was additionally flanked on both sides by tetranucleotide sequences (5′-ATCT-3′ and 5′-TTTA-3′), which increased the complementarity with the leader sequence to a total stretch of 17 nt. The expression cassettes were first inserted between the E and the M genes simply because it required a minimal number of cloning steps to construct the transcription vectors. The new junctions generated are indicated in Fig. 1, whereas their sequences are shown in Fig. 2. After confirmation of both constructs by restriction and sequence analyses, the recombinant viruses MHV-ERLM, containing the RL gene, and MHV-EFLM, containing the FL gene (Fig. 3A), were generated by homologous recombination between the genome of fMHV and donor RNA transcribed from the transcription vectors, as described earlier (9). fMHV is an MHV derivative in which the S ectodomain is replaced by that of FIPV. As a result, the virus is no longer able to grow in murine cells; it can only grow in feline cells. Due to the presence of the MHV S sequence in the donor RNA transcripts, recombinant viruses containing the foreign expression cassettes can simply be selected by their regained ability to grow in murine cells. The genotypes of the recombinant viruses were confirmed by RT-PCR on gRNA isolated after two rounds of plaque purification.

Intracellular RNA synthesis of MHV-ERLM and MHV-EFLM. To examine the patterns of viral RNA synthesis of MHV-ERLM and MHV-EFLM, infected cells were metabolically labeled with [^{33}P]orthophosphate in the presence of actinomycin D. Purified total cellular RNA was analyzed by electrophoretic separation (Fig. 3B). For the reconstructed wild-type virus (MHV-WT), the mobilities and relative amounts of the sgRNA species were similar to those observed previously (9, 10). For MHV-ERLM and MHV-EFLM, the expected additional sgRNA species were observed (RL-M-N and FL-M-N, respectively), whereas the sizes of all sgRNAs generated from TRSs located upstream of the foreign expression cassettes had increased proportionally. These sgRNAs were larger after insertion of the FL gene than after insertion of the RL gene, a finding consistent with the size difference of these luciferase genes. The sgRNA RL-M-N of MHV-ERLM migrated just ahead of sgRNA 4a/b-5a/E-M-N of MHV-WT (calculated size, 3.66 kb), as predicted by its theoretical size of 3.55 kb. For MHV-EFLM, the sgRNA FL-M-N (expected size, 4.31 kb) migrated in between sgRNAs 5a/E-RL-M-N and 4a/b-5a/E-RL-M-N of MHV-ERLM, which have calculated sizes of 4.19 and 4.59 kb, respectively. Two additional, unexpected RNA species were observed in cells infected with MHV-EFLM (FL* and FL** [see below]). Strikingly, the labeling intensities of the RL-M-N and FL-M-N sgRNAs differed profoundly, whereas the intensities of the other sgRNA species were more or less comparable. MHV-ERLM and MHV-EFLM differ only in the sequence downstream of the TRS in the inserted expression cassette. Apparently, the transcription levels of the sgRNAs can be affected by sequences downstream of the TRS, i.e., by the foreign gene itself. The results confirm the genotypes of the recombinant viruses and indicate that different foreign genes can be transcribed after insertion into the coronaviral genome.

We assumed that the additional smaller RNA species FL* and FL** observed for MHV-EFLM were sgRNA species originating from unintended leader-to-body fusion events that occur in regions in the FL gene with fortuitous homology to the leader. The identity of the additional RNAs was studied by RT-PCR on purified cellular RNAs, followed by sequence analysis. The RT-PCR strategy and the results are shown in Fig. 4A. For the analysis of FL*, the RT-step was performed with primer 1092 (9), which is complementary to a sequence in the 5′ end of the M gene, whereas the PCR was performed with primers 1495 and 1814, which are complementary to sequences in the 5′ end of the leader and in the 3′ end of the FL gene, respectively. A predominant RT-PCR product of ca. 0.75 kb was obtained. Sequence analysis showed that the leader was fused to the body of the sgRNA at a small stretch of homology between the leader sequence and the FL gene 920 nt downstream of the FL start codon (5′-AUCUAA-3′). The resulting sgRNA had a predicted size of 3.37 kb, which was slightly larger than the calculated size of the 5a/E-M-N sgRNA (ca. 3.28 kb) synthesized in cells infected with MHV-WT and corresponded with the electrophoretic mobility of RNA FL* (Fig. 3B). For the analysis of RNA FL**, a similar strategy was performed with primer 1814 in the RT step, whereas the PCR was performed with primers 1495 and 1828, the latter one corresponding to a sequence in the FL gene just upstream of the FL* leader-to-body fusion site. Two RT-PCR products of ca. 0.5 and 1.0 kb were obtained. Sequence analysis of the largest RT-PCR product showed that the leader was fused to the body of the sgRNA at the TRS in front of the FL gene, i.e., at the intended leader-to-body fusion site (designated FL^i) (Fig. 4A). In the smaller RT-PCR product, the leader was fused to the body of the sgRNA at a small stretch of homology (5′-UCUAAA-3′) between the leader sequence and the FL gene 462 nt downstream of the FL start codon. The predicted size of this sgRNA (ca. 3.83 kb) corresponded to the electrophoretic mobility of sgRNA FL** (Fig. 3A).

Although aberrant sgRNAs could not be observed by electrophoretic separation of metabolically labeled RNAs synthe-

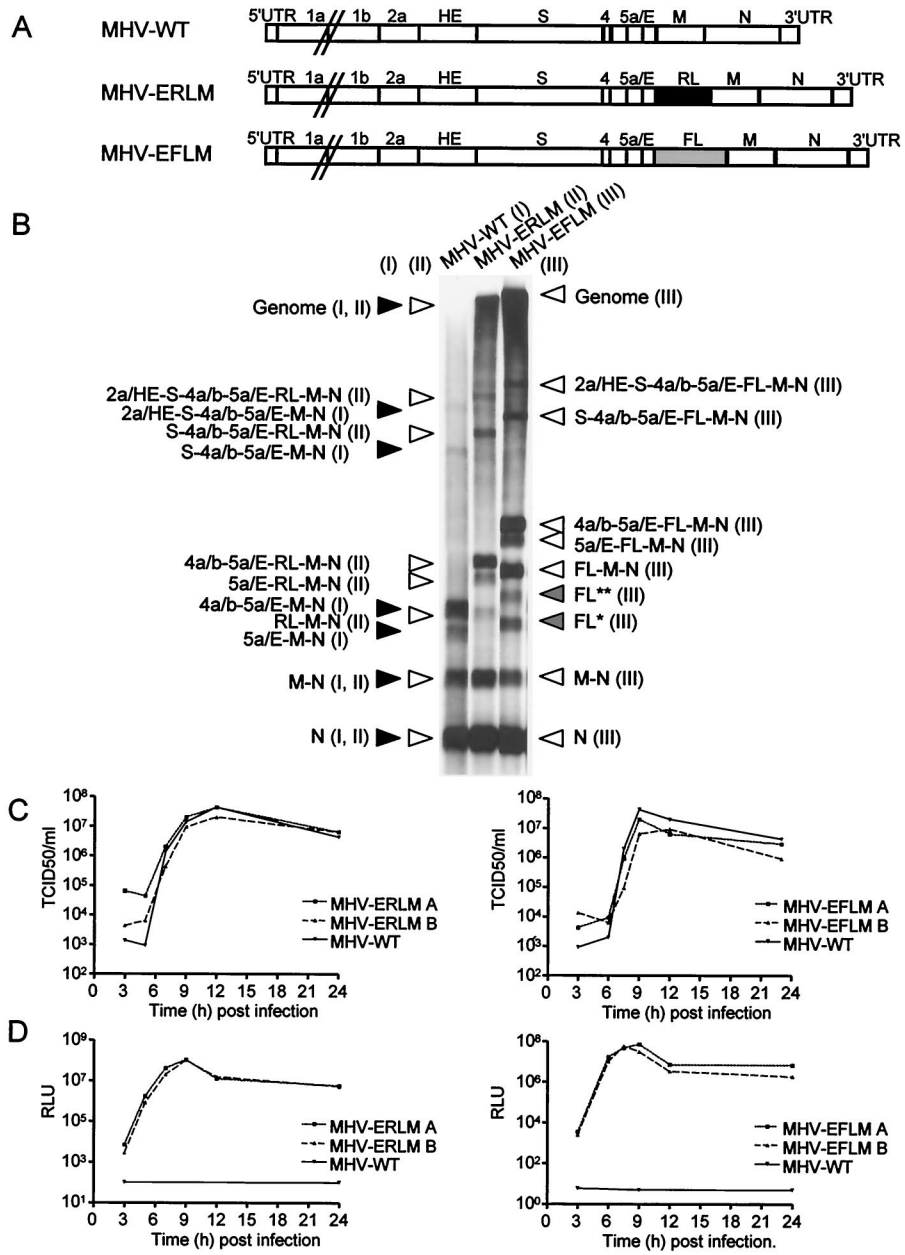

FIG. 3. Recombinant viruses with luciferase gene cassettes between the E and the M gene. (A) Genomic organization of the recombinant wild-type MHV-A59 (MHV-WT) and of the recombinants containing either an RL or an FL expression cassette between the E and M genes. (B) Intracellular RNA synthesis by the recombinant MHVs was analyzed as described in Materials and Methods. Purified total cytoplasmic RNA was separated by electrophoresis through 1% agarose containing formaldehyde, and labeled RNA was visualized by fluorography. The position of each RNA species is indicated by triangles alongside the panels. An I, II, or III in parentheses indicates the viral source of the RNA species as being MHV-WT, MHV-ERLM, or MHV-EFLM, respectively. (C) Single-step growth kinetics of the MHV recombinants. LR7 cells were infected with each recombinant MHV at an MOI of 8. Viral infectivity in the culture media at different times postinfection was determined by a quantal assay on LR7 cells, and $TCID_{50}$ values were calculated. Independently generated recombinants are indicated by the addition of A and B. (D) In a parallel experiment, the intracellular expression of RL and FL was determined at different times postinfection by using a luminometer (in RLU).

sized in cells infected with MHV-ERLM (Fig. 3B), a similar RT-PCR analysis was performed on cellular RNAs purified from these cells (Fig. 4B). The first RT step was performed with primer 1092, while the PCR was performed with primers 1495 and 1855, the latter being complementary to a sequence in the 3′ end of the RL gene. Two predominant RT-PCR products were observed of ca. 0.4 and 1.0 kb. Sequence analysis showed that in the largest RT-PCR product the leader was fused to the body of the sgRNA at the intended position (designated RL^i, i.e., the TRS in front of the RL gene; Fig. 4). In the smaller RT-PCR product the leader was fused to the body of the sgRNA at a small stretch of homology (5′-AUCU-

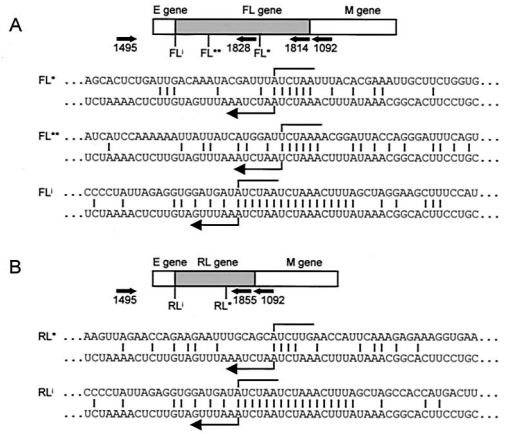

FIG. 4. PCR and sequence analysis of aberrant sgRNAs. RT-PCR was used to amplify regions of cytoplasmic RNA isolated from cells infected with MHV-EFLM (A) or MHV-ERLM (B). The approximate locations of primers 1092 (9), 1814 (5′-GGTACTTCGTCCACAAAC AC-3′), 1828 (5′-GGCGAAGAAGGAGAATAGG-3′), and 1855 (5′-GAGAACTCGCTCAACGAAC-3′) in the recombinant MHV genomes are shown. Primers 1092 and 1814 were used in the RT steps, whereas primer pairs 1814-1495, 1828-1495, and 1855-1495 were used for the PCR. The 3′ end of primer 1495 (5′-CCCGGGATCCATTTA GGTGACACTATAGAATATAAGAGTGATTGGCGTCC-3′) corresponds to the leader sequence of MHV. FL^i and RL^i indicate the intended leader-to-body fusion sites located just 5′ upstream of the FL and RL gene, respectively. FL*, FL**, and RL* indicate the aberrant leader-to-body fusion sites. The homology between the sequence of the fusion site (upper sequence) and the 5′ end of the genome (lower sequence) is marked by vertical bars. The arrows below the sequences indicate the sites of fusion of the body sequence to the leader sequence of the sgRNA.

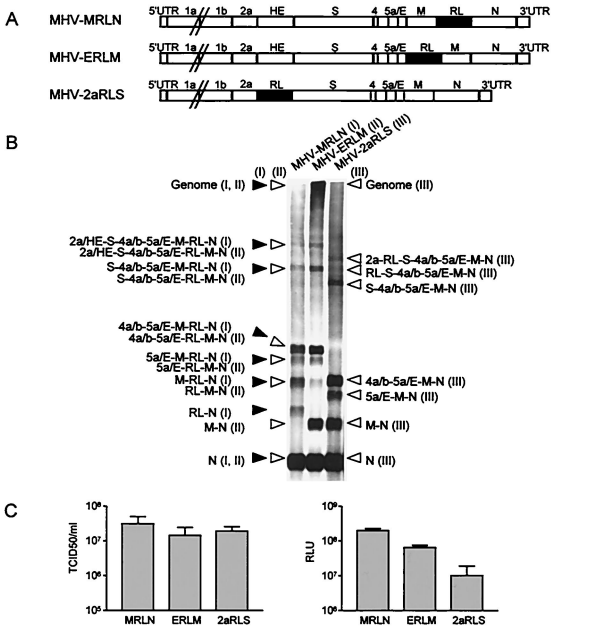

FIG. 5. Recombinant viruses with RL gene cassettes at different positions. (A) The genomic organization of the recombinant viruses containing the RL gene cassette between the M and the N genes (MHV-MRLN), between the E and the M genes (MHV-ERLM), and between the 2a and S genes is shown. (B) Intracellular RNA synthesis by the recombinant MHVs was analyzed as described in Materials and Methods and in the legend to Fig. 3. The position of each RNA species is indicated by triangles alongside the panels. An I, II, or III in parentheses indicates the viral source of the RNA species, i.e., MHV-WT, MHV-ERLM, or MHV-EFLM, respectively. (C) Titers and luciferase expression levels of the MHV recombinants at 9 h postinfection. LR7 cells were infected in quadruplicate with each recombinant MHV at an MOI of 8. Viral infectivity in the culture media was determined by a quantal assay on LR7 cells, and $TCID_{50}$ were calculated. In the same experiment the intracellular expression of RL (in RLU) was determined by using a luminometer; standard deviations are indicated.

3′) between the leader sequence and the RL gene 605 nt downstream of the RL start codon. Theoretically, this would correspond with an sgRNA of 2.97 kb (RL*).

In vitro growth and luciferase expression of recombinant viruses. The viral recombinants were analyzed for their in vitro growth characteristics. Pairs of independently generated recombinant viruses were taken to exclude the possibility that the observed phenotypes were a consequence of accidental, unintended mutations. The recombinant viruses appeared to behave very similar to MHV-WT with respect to syncytium formation, as well as for their one-step growth (Fig. 3C). All recombinant viruses reached high titers, although the yields of MHV-EFLM seemed slightly lower than those of MHV-WT. In a parallel experiment, the luciferase expressions were analyzed. All recombinant viruses, except MHV-WT, expressed high levels of either RL or FL, the enzymatic activities peaking at about 9 h postinfection (Fig. 3D). Luciferase expression could be demonstrated as early as 1.5 h postinfection (data not shown). Comparison with a standard curve of purified FL indicated that cells infected with MHV-EFLM expressed 1 to 2 μg of luciferase per 10^6 cells at 9 h postinfection (data not shown). The results demonstrated that insertion of a foreign expression cassette of 0.97 or 1.69 kb in length hardly affected the in vitro growth characteristics of the recombinant viruses and resulted in high levels of expression of the foreign genes.

Position-dependent expression of RL. A next set of recombinant viruses was constructed to study the genomic position dependence of foreign gene expression. RL expression cassettes, identical to the one positioned between the E and the M gene, were now inserted in the transcription vector between the M and the N gene (MHV-MRLN) and between the 2a and the S gene (MHV-2aRLS) (Fig. 1 and 5A). In the latter case the sequence of the HE pseudogene, which is not expressed in the A59 strain of MHV (27), was deleted. The new junctions generated are indicated in Fig. 1, and their sequences are shown in Fig. 2. The viruses were generated by targeted recombination and their genotypes were confirmed as described earlier.

The patterns of viral RNAs synthesized by MHV-MRLN and MHV-2aRLS were compared to that of MHV-ERLM. As is shown in Fig. 5B, the electrophoretic mobilities of the sgRNA species were as expected. For instance, sgRNA RL-N of MHV-MRLN migrated slightly more slowly than sgRNA M-N of MHV-ERLM, a finding consistent with the RL expression cassette being 274 nt larger than the sequence of the M gene, including its TRS. However, as predicted, the sgRNAs M-RL-N and RL-M-N, as well as all corresponding larger sgRNAs of MHV-MRLN and MHV-ERLM, comigrated. The sgRNA pattern of MHV-2aRLS was very similar to that of MHV-WT, with the exception of the additional sgRNA species

RL-S-4a/b-5a/E-M-N. The results confirm the genotypes of the recombinant viruses and show that the foreign expression cassette was transcriptionally active at each selected position in the viral genome.

For each type of recombinant virus, a pair of independently generated viruses was analyzed to study their phenotypes. After we established that in each case both viruses had very similar one-step growth curves and luciferase expression levels after a high-MOI infection (data not shown), we compared the different RL expressing viruses to each other (one of each pair). Since in all cases the luciferase expression levels peaked at about 9 h postinfection, this time point was chosen for the analysis. After a high-MOI infection of LR7 cells, the viral titers in the culture medium and the amount of luciferase activity in the cell lysates were determined. As shown in Fig. 5C, the different recombinant viruses all reached comparable high titers, indicating that the expression cassettes were tolerated at the different positions without affecting viral replication to an appreciable extent. However, the viruses differed significantly in their RL expression levels. The luciferase expression exhibited a clear position dependence, being increasingly higher as the inserted gene was closer to the 3′ end of the genome.

Insertion of foreign genes affects the expression from upstream TRSs. The genomic position dependence of foreign gene expression might be explained by an attenuating effect of downstream TRSs on the transcription from upstream TRSs (18, 20, 23, 45, 48). For this reason, it was of interest to study the effect of the insertions of the TRS/luciferase cassettes on the expression of the viral genes. It has been shown that the MHV structural proteins are synthesized in very similar relative ratios throughout the infection (35). LR7 cells were infected at a high MOI with the different recombinant viruses and labeled for 3 h with ^{35}S-labeled amino acids starting at 5 h postinfection. Subsequently, combined lysates of cells and culture media were prepared (8). These lysates were processed for immunoprecipitation with an anti-MHV serum that recognizes the major structural proteins S, M, and N, followed by SDS-PAGE. An example of such an experiment is shown in Fig. 6A for MHV-WT. The radioactivity in each protein was quantitated by phosphor scanning of the dried gels obtained from three independent experiments. The relative amounts of the proteins present in the cultures were determined and normalized to those of the wild-type virus, as described previously (10). Figure 6B shows that in cells infected with MHV-MRLN the S/N and M/N ratios were significantly decreased, whereas the S/M ratio was not appreciably altered. For MHV-ERLM, the M/N ratio was not altered, but the S/N and the S/M ratios were both significantly decreased. In MHV-2aRLS infected cells the protein ratios were not severely affected, although the S/N and S/M ratios were somewhat lower than those of MHV-WT. When cells were infected with MHV-EFLM, the S/N and S/M ratios were decreased, just as for MHV-ERLM, but now the M/N ratio was also lower. All observed changes were relatively small, i.e., twofold or less. In general, insertion of an expression cassette resulted in a lower relative expression of the genes located upstream of the cassette (S and M for MHV-MRLN; S for MHV-ERLM and EFLM), which is consistent with an attenuating effect of the downstream expression cassette on the transcription from upstream TRSs. In some cases

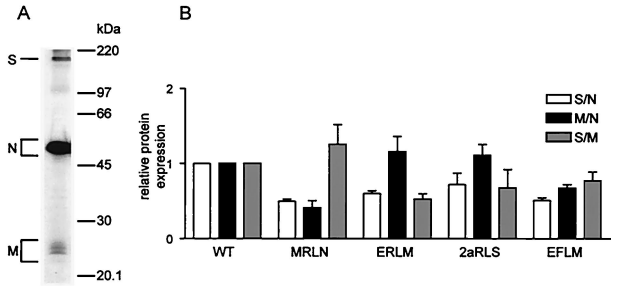

FIG. 6. Viral protein synthesis by different luciferase-expressing MHV recombinants. LR7 cells were infected with recombinant viruses and subsequently labeled with ^{35}S-labeled amino acids from 5 to 8 h postinfection. (A) Total lysates of cells and culture media were prepared and used for immunoprecipitation with the anti-MHV serum K134, and the precipitates were analyzed by SDS–15% PAGE. An example is shown for MHV-WT. The positions of the different viral proteins are indicated on the left, while those of molecular mass marker proteins are indicated on the right of the gel. (B) For quantitative analysis, the amounts of radioactivity in the M, S, and N proteins were determined by phosphorimager scanning of the dried gels from three independent experiments, with the indicated recombinant viruses. The ratios of the amounts of the S and N (S/N), M and N (M/N), and S and M (S/M) proteins synthesized in the cells infected with the luciferase-expressing viruses were calculated relative to those in MHV-WT-infected cells (set at 1.0); the standard deviations are indicated.

the relative expression of the gene located immediately downstream of the expression cassette was also decreased (S for MHV-2aRLS; M for MHV-EFLM).

Context versus position dependence of foreign gene expression. As concluded above, an inverse correlation appears to exist between the level of foreign gene expression and the distance of the expression cassette relative to the 3′ end of the genome. We were interested whether also the sequence context around the inserted cassette might somehow contribute to the expression level. We therefore generated a recombinant virus, MHV-ERLMSmN, in which the entire gene cluster 4a/b-5a/E-RL-M as it occurs in MHV-ERLM was moved to a position upstream of the S gene (Fig. 7A). As a result the distance of the RL gene relative to the genomic 3′ end was much larger than in the control virus MHV-ERLM, i.e., ca. 7.4 and 3.3 kb, respectively, whereas the immediate upstream and downstream sequences of the luciferase gene had remained the same. Thus, whereas the gene order in MHV-ERLM is 5′-replicase-2a/HE-S-4-5a/E-RL-M-N-3′, in MHV-ERLMSmN the genes occur in the sequence 5′-replicase-4-5a/E-RL-M-S-N-3′. In addition to the rearrangement of the gene order, the 2a and HE genes were deleted. We have shown previously that viruses from which the nonessential genes had been deleted or in which the gene order had been rearranged still replicated efficiently in vitro (9, 10). The genotype of the recombinant MHV-ERLMSmN virus was verified by RT-PCR analysis, and its RNA synthesis pattern was confirmed by radiolabeling and gel electrophoresis, which showed that the foreign expression cassette was transcriptionally active (data not shown).

Viral multiplication and luciferase expression levels of MHV-ERLM and MHV-ERLMSmN were compared in a one-step growth experiment. The results (Fig. 7B) show that the rearranged virus reached lower titers and expressed lower levels of luciferase at all time points. Since the stability and trans-

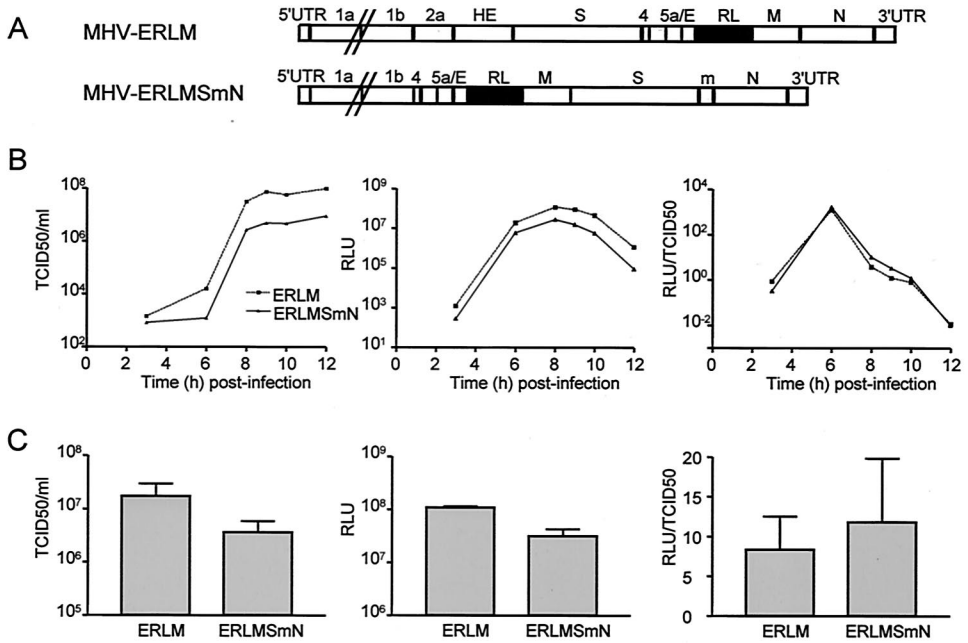

FIG. 7. Expression of RL from a virus with a rearranged genome. (A) Genomic organization of two recombinant viruses each containing the RL gene between the E and M genes: one in the context of a "normal" genome (MHV-ERLM) and the other in a genomically rearranged background (MHV-ERLMSmN). The "m" indicates a 126-nt segment from the 3′ end of the M gene. (B and C) LR7 cells were infected with each recombinant MHV at an MOI of 8. Viral infectivity in the culture media was determined by a quantal assay on LR7 cells either at different times (B, left graph) or at 9 h (C, left graph) postinfection, the latter in quadruple, and $TCID_{50}$ values were calculated. In the same experiment, the intracellular expression of RL was determined (in RLU) at the same times postinfection (B and C, middle graphs) by using a luminometer. The right panels of B and C show the RL expression as calculated relative to the virus titer (i.e., $RLU/TCID_{50}$). The standard deviations are indicated.

lational efficiency of the FL encoding sgRNAs of both viruses are likely to be similar, the luciferase expression levels (in RLU) can be considered as a direct measure of the FL sgRNA transcription levels. To correct for the difference in viral replication between the two viruses, we calculated the luciferase production at each time point relative to the actual viral titer ($RLU/TCID_{50}$). The curves thus obtained, shown in Fig. 7B (right panel), appear indistinguishable, indicating that the relative levels of luciferase expressed by both viruses are similar throughout the replication cycle. Interestingly, the highest value was obtained at 6 h postinfection, a time point at which the (extracellular) amount of virus just starts to rise, whereas the synthesis of luciferase is already nearing its maximum. A more detailed analysis of the relative luciferase expression was performed in an independent experiment carried out four times. Viral titers and luciferase expression were determined at 9 h postinfection, at which time these parameters have reached their maximal values. The results are shown in Fig. 7C. Again, MHV-ERLMSmN reached significantly lower titers and expressed significantly less luciferase. However, no significant difference in the relative luciferase expression level ($RLU/TCID_{50}$) was observed. The results indicate that the relative luciferase gene expression levels of the viruses do not differ, although the distance of their luciferase gene relative to the 3′ end of the genome differs by more than 4 kb. These results indicate that a reciprocal relationship between the distance of the luciferase gene relative to the 3′ end of the genome and the luciferase expression level does not necessarily exist.

Two foreign genes expressed from a single genome. Having established that two different luciferase genes can be expressed from different locations of the MHV genome, we next investigated whether simultaneous expression of the two genes from a single genome was also feasible. Therefore, the FL expression cassette was inserted between the E and the M genes in the transcription vector previously used to construct MHV-2aRLS (Fig. 1). Again, two independently generated recombinant viruses (MHV-RLFL; Fig. 8A) were generated, the genetic make-up of which was verified by RT-PCR. They expressed similar levels of FL and RL and reached similar titers after a high-MOI infection (data not shown). Next, the luciferase expression levels and the viral titers of MHV-RLFL were compared to those of MHV-2aRLS and MHV-EFLM (Fig. 8B). To this end, LR7 cells were infected in duplicate with the different recombinant viruses at high MOI. At 8 h postinfection, virus titers in the culture media were determined, and the intracellular RL and FL expression levels were measured. Figure 8 (left panel) shows that the recombinant viruses reached high titers, although those of the FL-containing viruses were somewhat lower (consistent with the results shown in Fig. 3C). Clearly, the presence of the RL gene in addition to the FL gene did not have a further negative effect on viral replication. While MHV-2aRLS and MHV-EFLM expressed only one type of luciferase, i.e., RL and FL, respectively, MHV-RLFL expressed both luciferases to a high extent. The results show that two foreign genes can be expressed efficiently

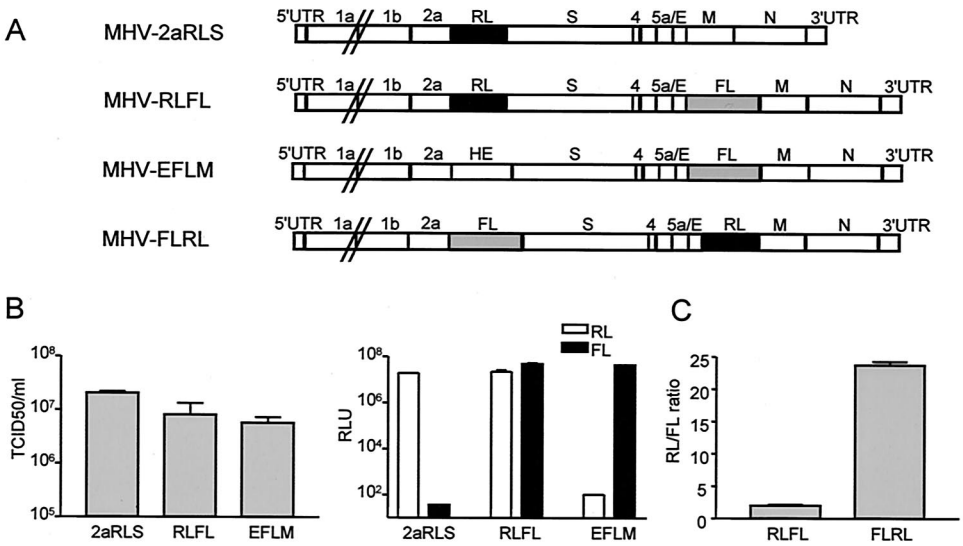

FIG. 8. Expression of RL and FL from a single genome. (A) The genomic organization of the recombinant viruses containing the RL gene between the 2a and S genes (MHV-2aRLS), the FL gene between the E and M genes (MHV-EFLM), or a combination thereof (MHV-RLFL) or containing the FL gene between the 2a and the S genes and the RL gene between the E and the M genes (MHV-FLRL) is shown. (B) Titers and luciferase expression of the MHV recombinants at 9 h postinfection. LR7 cells were infected in duplicate with each recombinant MHV at an MOI of 8. Viral infectivity in culture media was determined by a quantal assay on LR7 cells, and the $TCID_{50}$ values were calculated. In the same experiment the intracellular expression of RL and FL was also determined (in RLU). (C) Ratio of RL and FL luciferase expression (RL/FL ratio) of MHV-RLFL and MHV-FLRL. LR7 cells were infected as described above. At 8 h postinfection, the intracellular expression of RL and FL was determined, and the RL/FL ratio was calculated. The standard deviations are indicated.

from a single genome simultaneously, without severely affecting coronavirus viability.

In view of the observed position dependence of foreign gene expression, we finally investigated whether the RL and FL expression levels could be manipulated in a predictable way. To this end, we created a second dual expression virus similar to MHV-RLFL but in which the RL and FL expression cassettes had changed places. Based on our earlier findings this virus, MHV-FLRL (Fig. 8A), although containing the same expression cassettes as MHV-RLFL, was expected to have relatively lower FL but higher RL expression levels. Again, two independently generated recombinant viruses were generated, and their genotype and phenotype were verified. Next, the relative amounts of RL and FL expressed by MHV-FLRL were compared to those of MHV-RLFL (Fig. 8C). LR7 cells were infected in duplicate with the different recombinant viruses at a high MOI. At 8 h postinfection the two luciferase activities were measured, and the ratio of RL and FL expression (RL/FL ratio) was determined. As expected, the RL/FL ratio was much higher for MHV-FLRL than for MHV-RLFL. The results demonstrate again the position dependence of coronavirus foreign gene expression and show that expression levels can be manipulated in a rational way by inserting the foreign genes at specific positions in the coronavirus genome.

DISCUSSION

The results presented here demonstrate the potential of coronaviruses as viral vectors. Foreign genes appropriately inserted into the MHV genome and preceded by a TRS were efficiently expressed without significantly affecting the in vitro growth properties of the virus. Expression cassettes containing different, unrelated luciferase genes were successfully tested at several genomic positions, both individually and combined within a single MHV genome. The expression levels were dependent on the identity of the particular foreign gene, as well as on the insertion site, with expression being higher the closer that the gene was to the genomic 3′ end. The insertion of foreign genes was also combined with the deletion of nonessential genes and with the rearrangement of the conserved coronavirus gene order. While the deletion of nonessential genes has been shown to yield viruses that are attenuated in vivo but not in vitro (9; Haijema and Rottier, unpublished), rearrangement of the genome organization (10) aims to reduce the chances that recombination with virulent field virus will result in transfer of the foreign genes.

In view of their huge RNA genomes, their pleomorphic shapes, and their apparently variable sizes and of the extended helical nature of their nucleocapsids, coronaviruses are likely to accommodate large insertions of foreign sequences. In addition, the ability to delete several nonessential genes further expands this genetic space. By the combined insertion of the two luciferase gene cassettes, we showed that extension of the MHV genome by ca. 10% of its natural size (total insertion size of 2.7 kb) was indeed accepted without adverse effects on viral growth. Consistently, insertion of the GFP gene (0.7 kb) in TGEV or MHV genomes also had little effect on the in vitro replication characteristics (6, 13, 37) (44), the GFP-expressing MHVs being attenuated in their virulence (37). Although in our system luciferase expression levels of 1 to 2 $\mu g/10^6$ cells were obtained, GFP production levels of more than 40 $\mu g/10^6$ cells were achieved by using optimized TGEV vectors (12, 44). These amounts are quite similar to those observed for other positive-strand RNA virus vectors, such as poliovirus and car-

diovirus, but are significantly lower than those obtained with most alphavirus-based vectors, for which values of 50 to 300 $\mu g/10^6$ cells have been reported (see the review by Enjuanes et al. [12]).

As demonstrated here with MHV, foreign gene expression by coronaviruses is dependent on several conditions. One is the insertion site relative to the genomic 3′ end. As could most clearly be deduced from the RL activities expressed from different genomic positions (cf. MHV-MRLN, MHV-ERLM, and MHV-2aRLS), expression levels are generally higher when the foreign gene is inserted closer to the 3′ end of the genome. This relationship is, however, not necessarily linear since the effect is likely to be caused, at least in part, by the contribution of TRSs occurring between the expression cassette and the 3′ end rather than by the distance between the latter per se. Studies with DI-RNAs (20, 23, 45, 48) and full-length genomes (10, 18) have shown that downstream TRSs generally have an attenuating effect on the transcription from upstream TRSs. According to the prevailing theory TRSs function as transcriptional attenuators or terminators during negative-strand synthesis. Transcription either resumes at the same site or at the 5′ end of the positive template after a "jump" to the leader sequence (38, 39). Thus, the efficiency with which the RNA polymerase reaches a particular TRS decreases with the number of preceding TRSs. Accordingly, the luciferase expression levels we observed correlated inversely with the number of TRSs located downstream of the luciferase gene. Consistently, insertion of the luciferase expression cassettes in turn also had an attenuating effect on the relative expression of the viral genes located at more upstream positions.

Proximity of the heterologous gene to the 3′ end of the genome is, however, not the sole factor determining the efficiency of expression. The sequence context of the expression cassette is another important aspect. This was demonstrated most clearly when we compared the RL expression levels of MHV-ERLM and MHV-ERLMSmN. In these viruses the RL gene context is identical: the cassette is flanked by the M gene and by the gene cluster 4/5a/E at its 3′ and 5′ sides, respectively. However, the distance of the foreign gene with respect to the genomic 3′ end is very different (3.3 kb versus 7.4 kb). Nevertheless, the relative levels of luciferase activity expressed from the viruses appeared to be quite similar. Thus, the performance of MHV-ERLMSmN was not essentially affected by the positioning of the RL gene farther away from the 3′ end or by the consequent presence of an additional downstream TRS. The findings further show that the drastic genomic rearrangement realized in this vector is without severe consequences for the viability of the coronavirus, a finding consistent with our earlier observations (10).

Another important factor determining the expression level of an inserted gene cassette is the sequence context around the TRS. As was demonstrated in many studies with DI-RNAs (2, 3, 15, 19, 29, 33), flanking sequences can affect the transcriptional activity of a certain TRS, presumably by changing the local secondary or tertiary structure or by modulating RNA-protein interactions. Except when used in its natural genomic position the TRS of an inserted expression cassette will find itself in an artificial environment. The impact of the sequences upstream of the TRS will depend on the particular construct. Sequences flanking the core TRS (5′-AAUCUAAAC-3′) will, for instance, affect the complementarity with the leader sequence and thereby the transcriptional activity. The effects of upstream sequences may be negative or positive. This was demonstrated by a recombinant MHV in which transcription of the M gene appeared to be reduced by placing it immediately downstream of the S gene (10) and by another MHV in which three nucleotide changes introduced just upstream of the gene 4 TRS led to a strong increase in its transcriptional activity (9, 32). Consistently, insertion of foreign sequences may also alter the transcription of viral genes located immediately downstream of the insertion site. Examples thereof were observed here showing that the expression of the M and the S gene was decreased by the upstream presence of the luciferase gene in the cases of MHV-EFLM and MHV-2aRLS, respectively.

Also, sequences located downstream of a TRS can modify its transcriptional activity. Again, nucleotides immediately flanking the core sequence will do so by their direct effect on the complementarity with the leader sequence. However, the foreign sequences also contained in an expression cassette can affect their own expression by somehow influencing the TRS. This became clear when we compared the transcription patterns of the viruses MHV-ERLM and MHV-EFLM, which differ only in the identity of their luciferase genes. Dramatic differences were observed in the transcription levels of the mRNAs specifying the foreign genes, whereas the transcription of the viral mRNAs remained quite similar for the two viruses. How these foreign sequences exert these specific effects is not yet clear. It will, however, be important to gain more insight into this phenomenon since it should eventually allow prediction of foreign gene expression efficiencies, thereby enabling the rational design of future coronaviral vectors.

Besides the synthesis of the intended sgRNAs, insertion of foreign gene expression cassettes into coronavirus genomes has thus far almost invariably revealed the appearance of additional, smaller sgRNAs (13, 44) (the present study). These are the products of aberrant leader-to-body fusions that occur due to the occurrence of TRS-like sequences in the inserted gene. The unintended leader-to-body fusion sites in the FL and RL genes contained stretches of 6 or 4 nt homologous to the canonical TRS, respectively. Interestingly, identical stretches of sequence present in the MHV genome (21) and in a DI-RNA (29) have previously been shown not to direct the synthesis of sgRNAs. Apparently, the sequences flanking the unconventional leader-to-body fusion sites in the foreign genes have a positive effect (or lack an inhibitory effect) on the functioning of the TRS-like sequence. Alternatively, long-range RNA effects or processes involving the ribonucleoprotein interactions, as suggested by Fischer et al. (13), might play a role in determining the site of transcription initiation. Elimination of the TRS-like sequences, by mutations not affecting the encoded protein, might result in higher foreign gene expression levels as this is likely to reduce the attenuating effect of downstream TRS(-like) sequences on the expression from upstream TRSs.

Recently, genetic engineering of coronaviruses has become feasible by the availability of infectious cDNA clones (1, 5, 46, 49, 50) and by the development of efficient RNA recombination systems (14, 24). This allows us now to study the complex

interplay of factors determining sgRNA synthesis in the context of the complete genome. This is important because, whereas most data on coronavirus transcription have been generated by using DI-RNAs, these results may not always be directly applicable to full-length viral genomes (25). For the further evaluation of coronaviruses as vectors, an important issue will be the genetic stability of the viruses carrying foreign gene cassettes, since this will eventually determine the applicability of these vectors. While expression of the GFP gene was found to be stable in several coronaviruses (6, 13, 37, 44), our current studies with RL- and FL-expressing viruses indicate that the stable maintenance of foreign genes is dependent on the nature of the heterologous gene, on the particular coronavirus vector used, and on the particular site of gene insertion (C. A. M. de Haan, B. J. Haijema, and P. J. M. Rottier, unpublished results). Thus, while the RL gene was stably expressed from various genomic positions, the FL gene was much less stable, its expression being lost gradually through deletions in the FL expression cassette. Interestingly, moving the cassette to a more upstream position or inserting it in the FIPV genome resulted in a more stable phenotype.

ACKNOWLEDGMENTS

We thank Berend Jan Bosch and Bert Jan Haijema for stimulating discussions, David Boss for technical assistance in part of the work, and Iris de Haan for illumination.

This study has been carried out with financial support from the Commission of the European Communities, the specific RTD program "Quality of Life and Management of Living Resources," QLK2-CT-1999-00002, and "Generic Coronavirus Vaccine Vectors for Protection of Farm Animals against Mucosal Infections" to C.A.M.D.H. and P.J.M.R.

This study does not necessarily reflect the views of the Commission of the European Communities and in no way anticipates the Commission's future policy in this area.

REFERENCES

1. **Almazan, F., J. M. Gonzalez, Z. Penzes, A. Izeta, E. Calvo, J. Plana-Duran, and L. Enjuanes.** 2000. Engineering the largest RNA virus genome as an infectious bacterial artificial chromosome. Proc. Natl. Acad. Sci. USA **97:** 5516–5521.
2. **Alonso, S., A. Izeta, I. Sola, and L. Enjuanes.** 2002. Transcription regulatory sequences and mRNA expression levels in the coronavirus transmissible gastroenteritis virus. J. Virol. **76:**1293–1308.
3. **An, S., and S. Makino.** 1998. Characterizations of coronavirus *cis*-acting RNA elements and the transcription step affecting its transcription efficiency. Virology **243:**198–207.
4. **Bredenbeek, P. J., C. J. Pachuk, A. F. Noten, J. Charite, W. Luytjes, S. R. Weiss, and W. J. Spaan.** 1990. The primary structure and expression of the second open reading frame of the polymerase gene of the coronavirus MHV-A59; a highly conserved polymerase is expressed by an efficient ribosomal frameshifting mechanism. Nucleic Acids Res. **18:**1825–1832.
5. **Casais, R., V. Thiel, S. G. Siddell, D. Cavanagh, and P. Britton.** 2001. Reverse genetics system for the avian coronavirus infectious bronchitis virus. J. Virol. **75:**12359–12369.
6. **Curtis, K. M., B. Yount, and R. S. Baric.** 2002. Heterologous gene expression from transmissible gastroenteritis virus replicon particles. J. Virol. **76:**1422–1434.
7. **de Groot, R. J., R. J. ter Haar, M. C. Horzinek, and B. A. van der Zeijst.** 1987. Intracellular RNAs of the feline infectious peritonitis coronavirus strain 79–1146. J. Gen. Virol. **68:**995–1002.
8. **de Haan, C. A., L. Kuo, P. S. Masters, H. Vennema, and P. J. Rottier.** 1998. Coronavirus particle assembly: primary structure requirements of the membrane protein. J. Virol. **72:**6838–6850.
9. **de Haan, C. A., P. S. Masters, X. Shen, S. Weiss, and P. J. Rottier.** 2002. The group-specific murine coronavirus genes are not essential, but their deletion, by reverse genetics, is attenuating in the natural host. Virology **296:**177–189.
10. **de Haan, C. A., H. Volders, C. A. Koetzner, P. S. Masters, and P. J. Rottier.** 2002. Coronaviruses maintain viability despite dramatic rearrangements of the strictly conserved genome organization. J. Virol. **76:**12491–12502.
11. **de Vries, A. A. F., M. C. Horzinek, P. J. M. Rottier, and R. J. de Groot.** 1997. The genome organization of the *Nidovirales*: similarities and differences between arteri-, toro-, and coronaviruses. Semin. Virol. **8:**33–47.
12. **Enjuanes, L., I. Sola, F. Almazan, J. Ortego, A. Izeta, J. M. Gonzalez, S. Alonso, J. M. Sanchez, D. Escors, E. Calvo, C. Riquelme, and C. Sanchez.** 2001. Coronavirus derived expression systems. J. Biotechnol. **88:**183–204.
13. **Fischer, F., C. F. Stegen, C. A. Koetzner, and P. S. Masters.** 1997. Analysis of a recombinant mouse hepatitis virus expressing a foreign gene reveals a novel aspect of coronavirus transcription. J. Virol. **71:**5148–5160.
14. **Haijema, B. J., H. Volders, and P. J. Rottier.** 2003. Switching species tropism: an effective way to manipulate the feline coronavirus genome. J. Virol. **77:**4528–4538.
15. **Hiscox, J. A., K. L. Mawditt, D. Cavanagh, and P. Britton.** 1995. Investigation of the control of coronavirus subgenomic mRNA transcription by using T7-generated negative-sense RNA transcripts. J. Virol. **69:**6219–6227.
16. **Hofmann, M. A., R. Y. Chang, S. Ku, and D. A. Brian.** 1993. Leader-mRNA junction sequences are unique for each subgenomic mRNA species in the bovine coronavirus and remain so throughout persistent infection. Virology **196:**163–171.
17. **Hsue, B., T. Hartshorne, and P. S. Masters.** 2000. Characterization of an essential RNA secondary structure in the 3′ untranslated region of the murine coronavirus genome. J. Virol. **74:**6911–6921.
18. **Hsue, B., and P. S. Masters.** 1999. Insertion of a new transcriptional unit into the genome of mouse hepatitis virus. J. Virol. **73:**6128–6135.
19. **Jeong, Y. S., J. F. Repass, Y. N. Kim, S. M. Hwang, and S. Makino.** 1996. Coronavirus transcription mediated by sequences flanking the transcription consensus sequence. Virology **217:**311–322.
20. **Joo, M., and S. Makino.** 1995. The effect of two closely inserted transcription consensus sequences on coronavirus transcription. J. Virol. **69:**272–280.
21. **Joo, M., and S. Makino.** 1992. Mutagenic analysis of the coronavirus intergenic consensus sequence. J. Virol. **66:**6330–6337.
22. **Konings, D. A., P. J. Bredenbeek, J. F. Noten, P. Hogeweg, and W. J. Spaan.** 1988. Differential premature termination of transcription as a proposed mechanism for the regulation of coronavirus gene expression. Nucleic Acids Res. **16:**10849–10860.
23. **Krishnan, R., R. Y. Chang, and D. A. Brian.** 1996. Tandem placement of a coronavirus promoter results in enhanced mRNA synthesis from the downstream-most initiation site. Virology **218:**400–405.
24. **Kuo, L., G. J. Godeke, M. J. Raamsman, P. S. Masters, and P. J. Rottier.** 2000. Retargeting of coronavirus by substitution of the spike glycoprotein ectodomain: crossing the host cell species barrier. J. Virol. **74:**1393–1406.
25. **Lai, M. M., and D. Cavanagh.** 1997. The molecular biology of coronaviruses. Adv. Virus Res. **48:**1–100.
26. **Luytjes, W.** 1995. Coronvirus gene expression, p. 33–54. *In* S. G. Siddell (ed.), The *Coronaviridae*. Plenum Press, Inc., New York, N.Y.
27. **Luytjes, W., P. J. Bredenbeek, A. F. Noten, M. C. Horzinek, and W. J. Spaan.** 1988. Sequence of mouse hepatitis virus A59 mRNA 2: indications for RNA recombination between coronaviruses and influenza C virus. Virology **166:** 415–422.
28. **Makino, S., and M. Joo.** 1993. Effect of intergenic consensus sequence flanking sequences on coronavirus transcription. J. Virol. **67:**3304–3311.
29. **Makino, S., M. Joo, and J. K. Makino.** 1991. A system for study of coronavirus mRNA synthesis: a regulated, expressed subgenomic defective interfering RNA results from intergenic site insertion. J. Virol. **65:**6031–6041.
30. **Masters, P. S., C. A. Koetzner, C. A. Kerr, and Y. Heo.** 1994. Optimization of targeted RNA recombination and mapping of a novel nucleocapsid gene mutation in the coronavirus mouse hepatitis virus. J. Virol. **68:**328–337.
31. **Navas, S., S. H. Seo, M. M. Chua, J. D. Sarma, E. Lavi, S. T. Hingley, and S. R. Weiss.** 2001. Murine coronavirus spike protein determines the ability of the virus to replicate in the liver and cause hepatitis. J. Virol. **75:**2452–2457.
32. **Ontiveros, E., L. Kuo, P. S. Masters, and S. Perlman.** 2001. Inactivation of expression of gene 4 of mouse hepatitis virus strain JHM does not affect virulence in the murine CNS. Virology **289:**230–238.
33. **Ozdarendeli, A., S. Ku, S. Rochat, G. D. Williams, S. D. Senanayake, and D. A. Brian.** 2001. Downstream sequences influence the choice between a naturally occurring noncanonical and closely positioned upstream canonical heptameric fusion motif during bovine coronavirus subgenomic mRNA synthesis. J. Virol. **75:**7362–7374.
34. **Phillips, J. J., M. M. Chua, E. Lavi, and S. R. Weiss.** 1999. Pathogenesis of chimeric MHV4/MHV-A59 recombinant viruses: the murine coronavirus spike protein is a major determinant of neurovirulence. J. Virol. **73:**7752–7760.
35. **Raamsman, M. J., J. K. Locker, A. de Hooge, A. A. de Vries, G. Griffiths, H. Vennema, and P. J. Rottier.** 2000. Characterization of the coronavirus mouse hepatitis virus strain A59 small membrane protein E. J. Virol. **74:**2333–2342.
36. **Rottier, P. J., M. C. Horzinek, and B. A. van der Zeijst.** 1981. Viral protein synthesis in mouse hepatitis virus strain A59-infected cells: effect of tunicamycin. J. Virol. **40:**350–357.
37. **Sarma, J. D., E. Scheen, S. H. Seo, M. Koval, and S. R. Weiss.** 2002. Enhanced green fluorescent protein expression may be used to monitor murine coronavirus spread in vitro and in the mouse central nervous system. J. Neurovirol. **8:**381–391.
38. **Sawicki, D., T. Wang, and S. Sawicki.** 2001. The RNA structures engaged in

replication and transcription of the A59 strain of mouse hepatitis virus. J. Gen. Virol. **82:**385–396.
39. **Sawicki, S. G., and D. L. Sawicki.** 1990. Coronavirus transcription: subgenomic mouse hepatitis virus replicative intermediates function in RNA synthesis. J. Virol. **64:**1050–1056.
40. **Sawicki, S. G., and D. L. Sawicki.** 1998. A new model for coronavirus transcription. Adv. Exp. Med. Biol. **440:**215–219.
41. **Schaad, M. C., and R. S. Baric.** 1994. Genetics of mouse hepatitis virus transcription: evidence that subgenomic negative strands are functional templates. J. Virol. **68:**8169–8179.
42. **Sethna, P. B., S. L. Hung, and D. A. Brian.** 1989. Coronavirus subgenomic negative-strand RNAs and the potential for mRNA replicons. Proc. Natl. Acad. Sci. USA **86:**5626–5630.
43. **Siddell, S. G.** 1995. The *Coronaviridae*: an introduction, p. 1–10. *In* S. G. Siddell (ed.), The *Coronaviridae*. Plenum Press, Inc., New York, N.Y.
44. **Sola, I., S. Alonso, S. Zuniga, M. Balasch, J. Plana-Duran, and L. Enjuanes.** 2003. Engineering the transmissible gastroenteritis virus genome as an expression vector inducing lactogenic immunity. J. Virol. **77:**4357–4369.
45. **Stirrups, K., K. Shaw, S. Evans, K. Dalton, R. Casais, D. Cavanagh, and P. Britton.** 2000. Expression of reporter genes from the defective RNA CD-61 of the coronavirus infectious bronchitis virus. J. Gen. Virol. **81:**1687–1698.
46. **Thiel, V., J. Herold, B. Schelle, and S. G. Siddell.** 2001. Infectious RNA transcribed in vitro from a cDNA copy of the human coronavirus genome cloned in vaccinia virus. J. Gen. Virol. **82:**1273–1281.
47. **van der Most, R. G., R. J. de Groot, and W. J. Spaan.** 1994. Subgenomic RNA synthesis directed by a synthetic defective interfering RNA of mouse hepatitis virus: a study of coronavirus transcription initiation. J. Virol. **68:** 3656–3666.
48. **van Marle, G., W. Luytjes, R. G. van der Most, T. van der Straaten, and W. J. Spaan.** 1995. Regulation of coronavirus mRNA transcription. J. Virol. **69:** 7851–7856.
49. **Yount, B., K. M. Curtis, and R. S. Baric.** 2000. Strategy for systematic assembly of large RNA and DNA genomes: transmissible gastroenteritis virus model. J. Virol. **74:**10600–10611.
50. **Yount, B., M. R. Denison, S. R. Weiss, and R. S. Baric.** 2002. Systematic assembly of a full-length infectious cDNA of mouse hepatitis virus strain A59. J. Virol. **76:**11065–11078.